J. Eur. Opt. Society-Rapid Publ. 2023, **19**, 21

https://doi.org/10.1051/jeos/2023019
Available online at: https://jeos.edpsciences.org

Journal of the European Optical Society-Rapid Publications

Special Issue - EOSAM 2022
Guest editors: Patricia Segonds, Gilles Pauliat and Emiliano Descrovi

SHORT COMMUNICATION OPEN ACCESS

Switchable optics based on guided mode resonance in lithographically patterned vanadium dioxide with integrated heating layer

Markus Walther*, Thomas Siefke, Kristin Gerold, and Uwe D. Zeitner

Friedrich Schiller University Jena, Institute of Applied Physics, Albert-Einstein-Str. 15, 07745 Jena, Germany

Received 31 January 2023 / Accepted 13 April 2023

Abstract. Vanadium dioxide (VO_2) has promising applications in smart windows and active micro-optical devices due to its thermochromic properties. However, the successful fabrication and patterning of VO_2 thin films with the correct stoichiometry and phase are challenging. In this study, we investigated lithographically patterned and non-patterned VO_2 thin films fabricated by reactive ion beam deposition, using variable angle spectroscopic ellipsometry, Raman spectroscopy, and transmission and reflection measurements. The results show that the refractive index and extinction coefficient exhibit significant changes for near-infrared wavelengths when heated above 68 °C, confirming its thermochromic properties. The Raman spectroscopy results indicate the formation of the monoclinic phase VO_2(M) after annealing, which was not changed by reactive ion etching. Lithographically structured VO_2-layers were successfully realized demonstrating the potential of VO_2 as a material for active micro-optical devices, such as guided mode resonance filters with switchable reflectance. The results suggest that VO_2 has great potential as a promising material for actively switched optical elements and micro-optical devices.

Keywords: Vanadium dioxide, Guided mode resonance, Phase change material, Lithography, Switching, VO_2, Spectroscopy, Reflectivity, Reactive ion beam deposition, Micro optics.

1 Introduction

The reversible semiconductor to metal transition (SMT) of vanadium dioxide (VO_2) at a critical temperature of $T_{crit} = 68$ °C was first found in 1959 [1]. Since then, many potential applications were described, including, but not limited to, smart windows [2], adaptive optics [3], and optical switches [4, 5]. VO_2 thin films can be fabricated on different conductive and non-conductive materials [6]. The SMT is accompanied by a structural phase transition from the monoclinic low-temperature VO_2(M) to the rutile high-temperature VO_2(R) crystal structure [7], and several changes in physical properties, like the change in electrical resistivity, refractive index, and extinction coefficient, among others. However, the focus of most work is mainly on applications using non-patterned VO_2 or considering THz-radiation [8].

For this article, VO_2 thin films were deposited on silicon and fused silica substrates using reactive ion beam deposition (RIBD). On both types of samples, the VO_2 thin film was then lithographically patterned by reactive ion etching. The structural and optical properties of the films and the resulting gratings were studied using variable angle spectroscopic ellipsometry (VASE), Raman spectroscopy, transmission and reflection measurements.

We hereby propose the design for an actively switching reflector for the near infrared wavelength range with high switching ratio, that is based on guided mode resonances (GMR) in a lithographically patterned VO_2 grating structure. We use a one-dimensional grating with a period of 1 µm on a stack of conductive and nonconductive films (Fig. 1). The underlying layers serve as a resistive heating element to achieve the phase transition of vanadium dioxide. The heating element consists of a thin film of 20 nm ITO covered with 100 nm chromium contacts for the electrical connection to a regulated power supply. On top of the heating element is an electrically non-conductive film of 100 nm silicon dioxide (SiO_2). It insulates the heating element from the electrically conductive vanadium dioxide (VO_2) grating.

The aim of the optical design of the grating is to achieve a high switching ratio for reflected TE polarized light with a wavelength of $\lambda = 1550$ nm. At room temperature (below $T_{crit} = 68$ °C), incoming light is coupled into the waveguide structure formed by the grating itself and is absorbed.

* Corresponding author: walther.markus@uni-jena.de

2 Manufacturing

We developed a reactive ion beam deposition (RIBD) process for reproducibly manufacturing VO_2(M) layers of specified thicknesses ranging from less than 100 nm to over 400 nm. Using X-ray photoelectron spectroscopy (XPS) and Auger electron spectroscopy (AES), we were able to determine the stoichiometric composition and ratio of vanadium to oxygen of films depending on the oxygen partial pressure during the deposition. The partial pressure of oxygen was controlled by variation of the oxygen flow rate. After deposition, an annealing of the layer stack for 30 min at 520 °C in an atmosphere composed of nitrogen and oxygen in a 100:1 ratio and a total pressure of 10 mbar was performed. The formation of the phase VO_2(M) was validated by Raman spectroscopy. For all VO_2 thin films produced for this study we used this RIBD process to produce a consistent thickness after annealing of 300 nm for the resonant reflection grating and 265 nm for all other samples.

We fabricated four types of samples for our study. Two of these were non-patterned VO_2 thin films, one on a single side polished silicon wafer with <100> orientation and the other on a fused silica wafer coated with 20 nm ITO using a sputtering process. Additionally, we made two lithographically patterned VO_2 grating structures. One on a silicon substrate with no other thin films applied, and the other on fused silica substrate which had the proposed layer stack of Figure 1 applied. The chromium and silicon oxide films were deposited by ion beam deposition (IBD) and reactive ion beam deposition (RIBD), respectively. Both layers (Cr and SiO_2) were patterned individually by a lift-off process utilizing the negative tone resist AZ®nLOF 2070 (MicroChemicals). Afterwards, the VO_2 was deposited. To ensure, that the VO_2 is only present on the insulating SiO_2 areas we used another lift-off process prior to the annealing.

The VO_2 grating structures on both samples were created by first applying and patterning a chromium mask using e-beam lithography with positive tone resist FEP-171 (Fujifilm) and chlorine-based reactive ion etching (RIE). And afterwards by inductively coupled plasma (ICP) etching of the VO_2 layer against a chromium hard mask using carbon tetrafluoride. The chromium was later removed from the top of the ridges with RIE.

Each of the four samples were analysed by different means: ellipsometry, Raman and SEM analysis for the non-patterned thin film on silicon, temperature-dependent transmission measurements for the non-patterned thin film on fused silica, Raman analysis for the VO_2 grating on silicon, and reflection analysis for the VO_2 grating on fused silica.

3 Results

3.1 Complex refractive index of VO_2

The complex refractive index of the realized VO_2 thin films was measured using variable angle spectroscopic ellipsometry on samples deposited using RIBD on a bare silicon substrate. The refractive index (n) and extinction coefficient (k) were recorded at 25 °C and 90 °C, with temperature controlled by a regulated hot plate. The results of the measurements are shown in Figures 2a and 2b, respectively. It was observed that both, the refractive index and especially the extinction coefficient show a significant change for near infrared wavelengths.

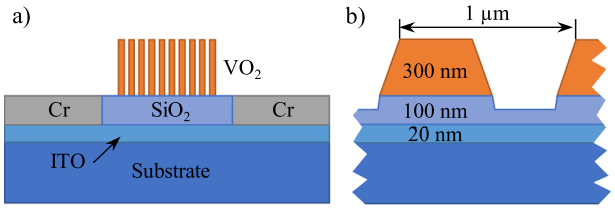

Fig. 1. (a) Design of the electrically switchable GMR-filter element. The ITO layer serves as resistive heating element underneath the VO_2 grating, which itself forms the waveguide structure. (b) Cross-sectional profile of GMR-filter element with dimensions.

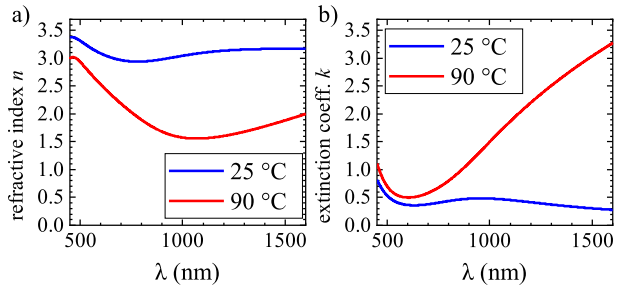

Fig. 2. (a) Refractive index n and (b) extinction coefficient k of prepared VO_2 film below and above the SMT.

3.2 Morphological changes

Scanning electron microscopy (SEM) images were analysed to detect structural and morphological changes of the deposited VO_2 thin films after the annealing and etching processes. The image in Figure 3a shows an amorphous layer directly after deposition. However, after the annealing process (see Fig. 3b), there is a formation of crystal grains with an average diameter of 56 nm with a $\sigma = 1.6$ nm, indicating a reorganization of the crystal structure. The annealing also led to a change in the thickness of the thin films from 226 nm before annealing to 265 nm after. This calculates to a film thickness increase of approximately 17%. While the first two images show samples with VO_2 on silicon substrate, the latter image shows the sample used for the reflection measurement that is described below. The etching depth into the thin film (see FIB-cut in Fig. 3c) was found to be not fully complete, with the grating not reaching its intended depth. Visible below the VO_2, there are 100 nm SiO_2 and 20 nm ITO. Please note, that for the preparation of the FIB-cut images there is chromium (mask material) and an additional layer of platinum on top of the grating. This was removed prior to other optical measurements.

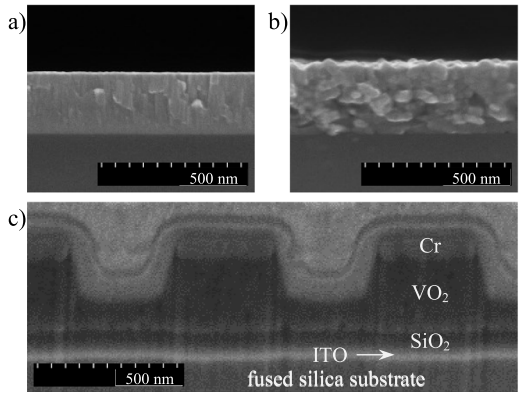

Fig. 3. SEM images of a cross-section of a VO_2 thin film on silicon substrate, (a) before annealing and (b) after annealing, indicating the growth of thickness. Image (c) shows an etched VO_2 grating with additional layers above and below. ITO is the thin bright layer above the substrate.

3.3 Crystalline phase

Raman spectroscopy was performed to identify the crystalline phase of VO_2 thin films on two different silicon samples. One after deposition as well as after annealing, and the other sample after etching the grating structure. The spectra (see Fig. 4) measured before and after the annealing process show the appearance of many characteristic peaks in accordance with other publications [9], implying the reconfiguration of the thin film to form the crystalline phase of VO_2(M).

Most prominent are two sharp peaks of VO_2(M) at 194 cm^{-1} and 224 cm^{-1} and the broader peak at 612 cm^{-1}. The peak at 520 cm^{-1} is due to the Si substrate material. This peak was particularly pronounced after etching, as the grating structure was opened to the underlying silicon. Other smaller peaks that are characteristic for VO_2(M) are marked with diamond (◆) shapes. The Raman spectroscopy measurements confirmed the formation of the monoclinic phase VO_2(M) after annealing and indicate that this phase was not changed by the etching process.

3.4 Transmittance

The transmission was measured at $\lambda = 1550$ nm on a non-patterned VO_2 sample with thickness of 265 nm (Fig. 5) on a fused silica substrate coated with an ITO heating layer. The sample was heated by applying a current to the resistive heating element directly in contact to the VO_2 thin film. The temperature T was calculated from the coupled electrical power assuming an ohmic resistance, a thermal system in equilibrium and two known points of reference. For no heating power, the temperature was 25 °C and the temperature of the SMT was found from previous experiments on a regulated hotplate and in accordance with literature [1] at 68 °C. At thermal equilibrium, the coupled power P_{heat} and the thermally radiated power P_{radiate} are equal, whereby the proportionality $P \sim T^4$ applies.

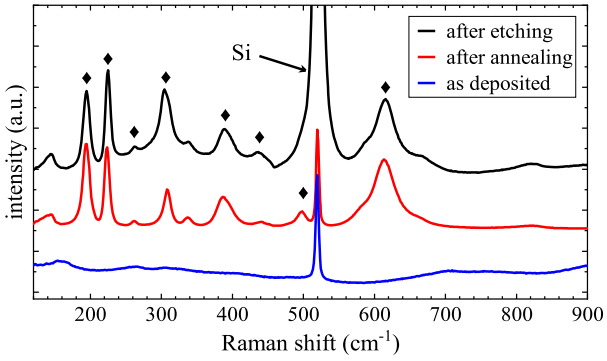

Fig. 4. Raman spectra of VO_2 films on Silicon: after deposition, after annealing and after etching (lines from bottom to top).

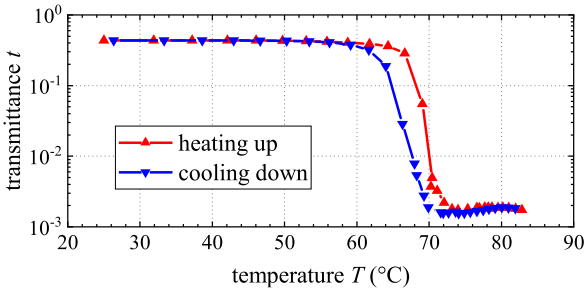

Fig. 5. Transmitted amplitude of the optical element in relation to the calculated temperature from heating power inserted into the resistive heating film. Each measurement was taken after thermal equilibrium was reached.

This way, a hysteresis with a width of $\Delta T \approx 4$ K could be observed. Depending on the applied heating current and resulting temperature, the transmittance could be actively switched between $t = 43.6\%$ and $t = 0.17\%$ multiple times, resulting in a transmission ratio of $c_t > 250$, which is in good agreement with the expected switching ratio of $c_t = 375$ according to RCWA.

3.5 Reflectance

The reflection properties of a VO_2 grating structure on fused silica substrate with additional layers as shown in Figure 1 were measured between 1460 nm and 1600 nm (see Fig. 6). This measurement was conducted below and above the SMT. By heating the sample to $T \approx 90$ °C, the reflectance can be actively controlled to a highly reflective state with $r = 51.7\%$ at a wavelength of $\lambda = 1580$ nm. At a temperature below the SMT ($T \approx 30$ °C), the reflectance significantly drops to $r = 0.77\%$. This results in a switching ratio of $c_r = 67$. The theoretical reflection calculated from the model in Figure 1 using RCWA is shown as dashed lines in Figure 6. Overall, the trend is followed closely, with deviations resulting mostly from the VO_2 not being fully opened, thereby degrading its performance. Despite the imperfect etching process, it could be demonstrated that VO_2 still exhibits thermochromic phase change after

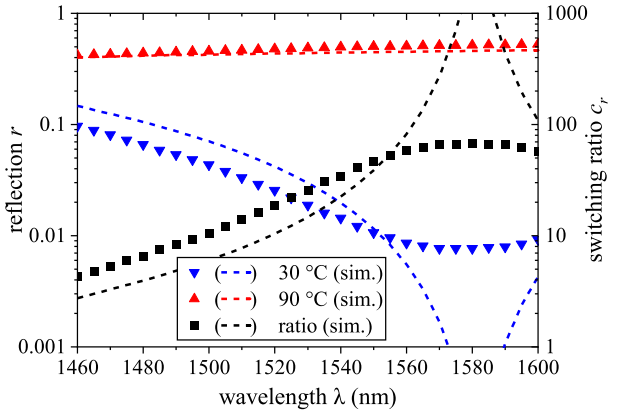

Fig. 6. Reflection of the guided mode resonance grating at 30 °C and 90 °C, respectively. The dashed lines show the results of RCWA simulation. The calculated reflection switching ratio c_r is shown in black.

ICP-etching and can be utilized to actively switch micro-optical devices.

4 Conclusion

In summary, we successfully fabricated and patterned VO_2(M) thin films using reactive ion beam deposition, e-beam lithography, and inductively coupled plasma etching, demonstrating the potential of VO_2 in micro-structuring, nano-optics, and guided mode resonant gratings. This article presented the design and fabrication of an actively switchable reflector based on guided mode resonances. The thermochromic properties of the material were verified through ellipsometry, transmission and reflection measurements and Raman spectroscopy measurements, which confirmed the presence of the monoclinic phase of VO_2(M) after annealing and showed its stability after ICP-etching.

However, deviations between the measured and theoretical reflection was observed, indicating that the VO_2 was not fully opened during etching. This shows the need for an optimized fabrication process to achieve the full potential of VO_2 in optical applications. One possible solution is to replace the SiO_2 layer with a more etch-resistant Al_2O_3 layer, which can serve as an effective etch-stop.

Despite the observed deviations, the thermochromic phase change and the ability to actively switch micro-optical devices after ICP-etching demonstrates the significant and versatile role of VO_2 in optical technologies. This creates new opportunities for the use of VO_2 in various micro-optical devices and systems, such as optical switches, filters, modulators, and more, making it a promising material for future advancements in the field of active optics and it paves the way for future studies in this field.

Conflict of interest

The authors declare no conflict of interest.

Acknowledgments. The authors acknowledge the financial support by the Federal Ministry of Education and Research (BMBF) of Germany and VDI (funding no. 13N15175). This work is funded through the project 20IND04 ATMOC within the Programme EMPIR. The EMPIR initiative is co-founded by the European Union's Horizon 2020 research and innovation program and the EMPIR Participating Countries.

References

1 Morin F.J. (1959) Oxides which show a metal-to-insulator transition at the Neel temperature, *Phys. Rev. Lett.* **3**, 34.
2 Gong X.Q., Li J.X., Chen S.Y., Wen W.J. (2009) Copolymer solution-based "smart window", *Appl. Phys. Lett.* **95**, 251907.
3 Rini M., Cavalleri A., Schoenlein R.W., López R., Feldman L.C., Haglund R.F., Boatner L.A., Haynes T.E. (2005) Photoinduced phase transition in VO_2 nanocrystals: Ultrafast control of surface-plasmon resonance, *Opt. Lett.* **30**, 558.
4 Ben-Messaoud T., Landry G., Gariépy J.P., Ramamoorthy B., Ashrit P.V., Haché A. (2008) High contrast optical switching in vanadium dioxide thin films, *Opt. Commun.* **281**, 6024.
5 Xu Z., Qin G., Bernussi A.A., Fan Z. (2021) Electrothermally control of dynamic infrared switching of VO_2 thin film on FTO glass, *J. Alloys Compd.* **858**, 157640.
6 Montero J., Ji Y., Li S., Niklasson G.A., Granqvist C.G. (2015) Sputter deposition of thermochromic VO_2 films on In_2O_3: Sn, SnO_2, and glass: Structure and composition versus oxygen partial pressure, *J. Vac. Sci. Technol. B* **33**, 031805.
7 Becker M.F., Buckman A.B., Walser R.M., Lépine T., Georges P., Brun A. (1994) Femtosecond laser excitation of the semiconductor-metal phase transition in VO_2, *Appl. Phys. Lett.* **65**, 1507.
8 Zhang D., Zhang Z., Liu W., Yu T. (2022) Switchable dual-functional guided-mode resonant filters based on VO_2 phase transition, *Opt. Mater. Express* **12**, 2288–2296.
9 Shvets P., Dikaya O., Maksimova K., Goikhman A. (2019) A review of Raman spectroscopy of vanadium oxides, *J. Raman Spectrosc.* **50**, 1226–1244.